Molecular Immunology 184 (2025) 13–21

Contents lists available at ScienceDirect

Molecular Immunology

journal homepage: www.elsevier.com/locate/molimm

CRISPR-Cas9 engineering of human T regulatory cells – Design and optimization of a manufacturing process

Ortal Shimon [a,b], Adam M. Dean [a,b], Shoshana Cohen [c], Aiden L. Moser [a], Clifford C. Dacso [a,b,d,e], Yosi Gilad [a,b,*], David M. Lonard [a,b,d,*], Bert W. O'Malley [a,b,d,*]

[a] Department of Molecular and Cellular Biology, Baylor College of Medicine, Houston, TX, United States
[b] CoRegen, Inc., Baylor College of Medicine, Houston, TX, United States
[c] SC Bioinformatics Consulting Group, Givat Shmuel, Israel
[d] Nuclear Receptor, Transcription and Chromatin Biology Program, Dan L. Duncan Cancer Center, Baylor College of Medicine, Houston, TX, United States
[e] Department of Medicine, Baylor College of Medicine, Houston, TX, United States

A B S T R A C T

Regulatory T cells (Tregs) are a subset of CD4 + T cells that comprise 5–10 % of the total CD4 + T cell population. Tregs, which are critically important for the maintenance of immune tolerance and immune homeostasis, are distinguished from other subtypes of CD4 + T cells by the expression of the transcription factor FOXP3. Because of the centrality to immunoregulation, Tregs have gained increasing attention as promising targets for clinical applications in autoimmune diseases, transplant rejection and graft-versus-host disease (GvHD). However, the essential role of Tregs in the complex network of the immune system implies their targeting as a promising therapeutic approach also in other medical indications, such as neurodegenerative diseases and cancer. Our group recently published a study showing that genetically modified Tregs are capable of clearing solid malignancies in various mice models, including an aggressive triple negative breast cancer (TNBC) and prostate cancer, which provides the impetus to develop an adoptive cell therapy using Steroid Receptor Coactivator 3 (SRC-3) knock out (KO) Tregs. It is well known that isolation, genetic editing and the expansion of Tregs as a homogenous and healthy population present specific technical challenges. In this context, here we outline the development of a process for the production of SRC-3 KO human Tregs (hTregs), which can subsequently be adapted for Current Good Manufacturing Practice (cGMP) settings to facilitate clinical-scale production.

1. Introduction

Properly functioning Tregs within the complex network of the immune system are critically important for the maintenance of self-tolerance and immune homeostasis. Loss of Treg-mediated immunosuppressive activity leads to severe autoimmune disorders, including neuroinflammation and neurodegenerative conditions (Kleinewietfeld and Hafler, 2014; Machhi et al., 2020; Liston et al., 2024). The ability of Tregs to establish a tailored and durable immune suppression makes Treg-based cellular therapy an attractive alternative to conventional immunosuppressants, such as small molecule-drugs and antibodies, for restoring self-tolerance in autoimmune diseases and achieving immunosuppression in organ transplantation settings (Bluestone et al., 2023; Ferreira et al., 2019). In cancer, Tregs are usually associated with disease progression, since their immunosuppressive activity largely contributes to immune evasion of cancer cells (Togashi et al., 2019).

The establishment of the clustered regularly interspaced short palindromic repeats (CRISPR)-Cas-based technology as a feasible, powerful and versatile gene-editing tool, has significantly facilitated genetic manipulations including in primary immune cells, which has expanded the potential for next generation cellular therapies, fundamentally transforming the research and development in this field (Chen et al., 2023). A unique example that introduces a promising opportunity of utilizing genetically engineered Tregs for the treatment of solid cancers has been recently reported by our laboratory (Han et al., 2023). SRC-3 plays a regulatory role across various immune cells and is particularly crucial for the proliferation, development, and function of lymphoid cells (Gilad et al., 2022, 2024). Additionally, SRC-3 is highly expressed in Tregs and plays an essential role in supporting their immune-suppressive functions (Nikolai et al., 2021). We showed that a conditional KO (cKO) of SRC-3 in Tregs promotes the development of local anti-tumor immunity within the tumor microenvironment (TME), which eventually leads to tumor clearance (Han et al., 2023). While CRISPR-Cas gene editing technology has facilitated genetic manipulations, given the scarcity and relative fragility of Tregs, the ability to attain a sufficient population of effectively edited, healthy Tregs presents a technical challenge for their clinical application (Raffin et al., 2020). Driven by our recently published data that potentiates the

* Corresponding authors at: Department of Molecular and Cellular Biology, Baylor College of Medicine, Houston, TX, United States.
E-mail addresses: yosi@bcm.edu (Y. Gilad), dlonard@bcm.edu (D.M. Lonard), berto@bcm.edu (B.W. O'Malley).

https://doi.org/10.1016/j.molimm.2025.05.019
Received 30 December 2024; Received in revised form 21 May 2025; Accepted 22 May 2025
Available online 4 June 2025

development of SRC-3 KO Treg-based anti-cancer cell therapy, here we describe a process development for isolation, editing and expansion of SRC-3 KO hTregs that can then be transferred to a cGMP set up.

2. Results

2.1. Selection of sgRNA

Selection of an optimal single guide RNA (sgRNA) for the production of a genetically edited cell therapy is critical for achieving a viable population of effectively, on-target edited cells with minimal off-target edits. Four synthetic sgRNAs that target the *NCOA3* gene, encoding for SRC-3, were selected from Synthego's catalog (Table S1): sgRNA1 was the top overall pick according to vendor's algorithm, sgRNA2 had the highest on-target score and sgRNAs 3 and 4 target the two key functional exons of *NCOA3* - 11 and 12 respectively (Han et al., 2023; Liu et al., 2008). A preliminary KO efficiency test in Jurkat cells indicated that sgRNAs 2, 3 and 4 most efficiently reduce the mRNA levels of *NCOA3* (Fig. 1a). Since sgRNAs 3 and 4 target the largest and most important exons of this gene, we continued with their evaluation in the target cells, utilizing a previously described CRISPR-Cas9-based gene KO procedure (Stadtmauer et al., 2020). hTregs were isolated from leukapheresis products (leukopaks or buffy coats, Table S8) using magnetic beads to first deplete CD8 + and CD19 + cells followed by enrichment of the CD25 + population. Although CD127 is frequently utilized to further refine Treg isolation by excluding activated conventional T cells, given that some activated Tregs also express CD127 (Simonetta et al., 2010), and considering the relative scarcity of Tregs and the need for sufficient cell numbers for downstream applications, in this study we chose to avoid CD127-based selection in order to optimize cell yield. For similar reasons we did not use CD45RA-based selection, which is a well-established marker for naïve Tregs and is often favored in therapeutic applications involving immunosuppression where high lineage stability is critical (Miyara et al., 2009). The resulting enriched $CD4^{+}CD25^{+}$ T cells were then nucleofected with ribonuclear protein (RNP) complexes containing specific sgRNAs (3 or 4). Subsequently, the cells were subjected to TCR stimulation for four-days, after which they were cultured in an anti-CD3/-28-free media and harvested at indicated time points (materials and methods) for protein, RNA and DNA isolation. While both sgRNAs effectively reduced SRC-3 protein levels in hTregs, sgRNA4 was more effective in reducing *NCOA3* mRNA levels, as indicated by RTqPCR (Fig. 1b, S1a, b) and further supported by Tracking of Indels by Decomposition (TIDE) analysis (Fig. 1c, S1c, Table 1, S2). For evaluation of the off-target effects we implemented two orthogonal sequencing methods: Genome-wide Unbiased Identification of Double strand breaks (DSBs) Enabled by Sequencing (GUIDEseq) and Primer-Extension-Mediated Sequencing (PEM-Seq) analyses. GUIDEseq utilizes a cell-based assay and can sensitively detect off-target cleavages (Tsai et al., 2015). GUIDEseq is based on the incorporation of double-stranded oligodeoxynucleotides (dsODNs) in DSBs followed by the non-homologous end joining (NHEJ) DNA repair pathway. The integrated dsODNs are later amplified to detect and quantify the off-target effects. This technique enables the detection of all high-frequency unexpected cutting sites created by CRISPR-Cas9 in cells. GUIDEseq was found to detect genuine nuclease off-target sites with an indel frequency as low as 0.2 %, which is approaching the typical limit of detection (LOD) (0.1 %) by next generation sequencing (NGS) (Liang et al., 2022). hTregs were isolated from three healthy human donors and nucleofected with dsODNs and the sgRNA-Cas9 RNP complex. The nucleofected hTregs were analyzed five days and 14 days after nucleofection. As expected, the on-target sequence was found with the highest number of reads for all samples, followed by three identical off-targets found in all three donors for sgRNA3 (Figure S1d), and four identical off-targets found in all three donors for sgRNA4 (Figure S1e). All samples had > 50,000 on-target reads, well above the threshold, to detect 0.1 % off-target sites relative to the on-target. sgRNA4 had more off-targets overall (44–67) compared to sgRNA3 (12–30), as well as higher percentage of read counts associated with these off-targets. Only ~55 % of all aligned reads for sgRNA4 were on-target compared to ~96 % of on-target reads in sgRNA3 (Table 2). However, only seven off-targets

Table 1
Summary of editing efficiency of sgRNAs 3 and 4 in human Tregs from donor 2342 as was evaluated by TIDE analysis.

	sgRNA3		sgRNA4	
Primer	Editing efficiency	AV Edit efficiency	Editing efficiency	AV Edit efficiency
Forward (F)	59.2 %	53.5 %	94 %	93.8 %
Revers (R)	47.4 %		93.6 %	

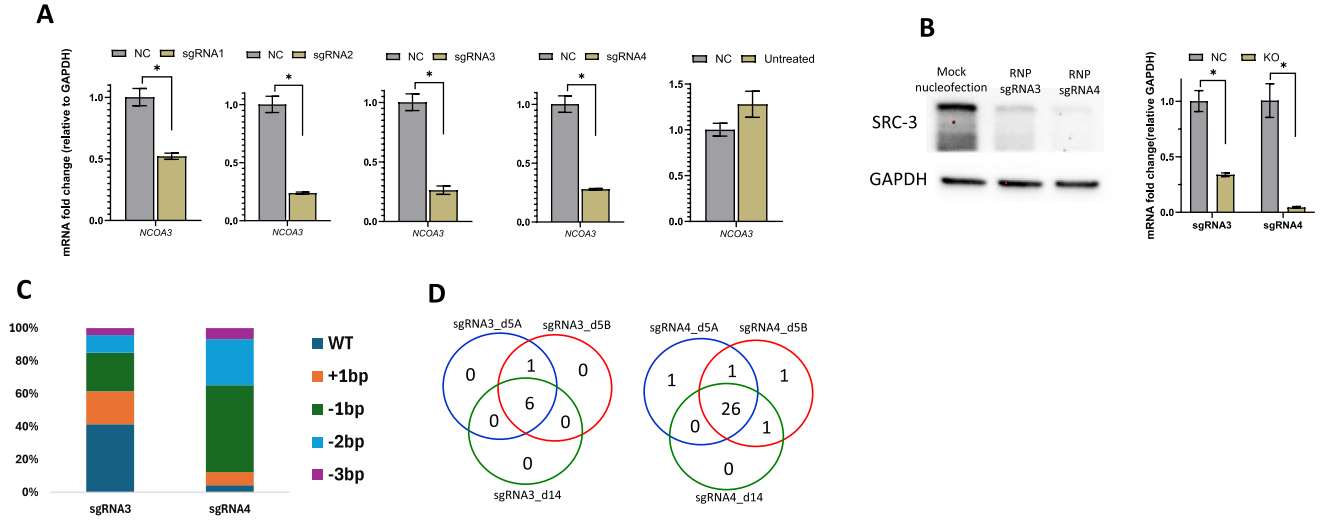

Fig. 1. Editing efficiency of sgRNAs 1–4 in Jurkat cells as was evaluated by RTqPCR (A). Editing efficiency of sgRNAs 3 and 4 in hTregs from donor 2407 as was evaluated by RTqPCR (right) and western blot (left). Representative data of at least two independent experiments showing similar results (B). Editing efficiency of sgRNA 3 and sgRNA4 in hTregs from donor 2342 as was evaluated by TIDE analysis (C). Overlap of off-target events passing the 0.1 % filter found by GUIDEseq in sgRNA3 (left) and sgRNA4 (right) samples. Sample d5A = donor 2322, five days after nucleofection; Sample d5B = donor 2330, five days after nucleofection; Sample d14 = donor 2424, 14 days after nucleofection (D). *P < 0.05, paired two-tailed *t*-test.

Table 2
Summary of on- and off-target events found by GUIDEseq in sgRNAs 3 and 4. Sample d5A = donor 2322, five days after nucleofection; Sample d5B = donor 2330, five days after nucleofection; Sample d14 = donor 2424, 14 days after nucleofection.

Donor	2322	2330	2424	2322	2330	2424
sgRNA-sample	**sgRNA3-d5A**	**sgRNA3-d5B**	**sgRNA3-d14**	**sgRNA4-d5A**	**sgRNA4-d5B**	**sgRNA4-d14**
On-target % reads from total reads	96.36 %	95.86 %	99.39 %	55.44 %	53.64 %	68.93 %
Off-target events	18	30	12	44	67	53
Off target events in oncogenes	1	1	1	2	4	2
Off target events in exons	0	2	0	1	2	0
Off target events > 0.1 %	6	4	3	23	27	13
Off target events > 0.1 % in oncogenes	1	0	0	1	0	1
Off target events > 0.1 % in exons	0	0	0	0	0	0

passed the 0.1 % editing relative to on-target editing LOD for sgRNA3, and 29 targets passed for sgRNA4. All off-targets had a near-perfect overlap between all replicates for both sgRNAs (Fig. 1d). Importantly, of these off-targets passing the 0.1 % threshold, none were found to be in exons. In sgRNA3 one off-target was found to be in the intron of a tumor suppressor gene (TSG), *DCUN1D3*, at 0.16 % editing relative to the on-target reads. In sgRNA4 one off-target was found to target an intron of the oncogene *ADAM9* at a ratio of 0.18 % editing relative to the on-target (Table S3). Importantly, for both guides the day 14 GUIDEseqs had fewer off-targets than the day five GUIDEseqs, indicating low survival rate of cells with high frequency of off-target editing.

GUIDEseq identifies repaired DSB junctions, but it does not detect structural rearrangements such as translocations, inversions, and large deletions. Complementary methods to identify structural rearrangements such as PEM-Seq are used to comprehensively identify and quantify editing events (Liu et al., 2022). PEM-Seq is a high-throughput sequencing method that can fully assess the specificity of engineered nucleases as well as their editing ability. With this method, chromosomal translocations and large deletions also can be detected. Simultaneously, on-target editing efficiency can be assessed. PEM-seq can sensitively detect CRISPR/Cas9 cutting sites and assess their editing efficiency by quantifying imperfect Cas9-induced DSB repair products (Liu et al., 2022). hTregs from a healthy donor were nucleofected with an RNP complex of either sgRNA3 or sgRNA4. The off-target events and editing efficiency were evaluated using PEM-Seq analysis after 14 and 30 days post-nucleofection, to allow sufficient time for translocation events to occur and stabilize. Editing efficiency for sgRNA3 for days 14 and 30 was 64 % and 54 %, respectively and for sgRNA4 87 % and 82 %, respectively (Table 3). Overall, PEM-Seq on-target editing results were consistent with TIDE analysis (Table S4) and RTqPCR data - all methods showed successful on-target editing for both guides, while sgRNA4 possessed higher editing efficiency. As expected, due to the lower editing efficiency of sgRNA3, there were ~30 % more wild type (WT) reads in the sgRNA3 sample compared to the sgRNA4 sample (Table S5). Insertions, inversions and translocations were similar (within x2 fold change) between the guides, with the exception of inversions within chromosomes located less than 500 kb away from the cut-site, which was nearly an order of magnitude more in sgRNA4 (x8.4 fold) compared to sgRNA3 (Table S5). When we filtered for samples with minimum reads > 2, sgRNA alignment of + /-50bp to the junction site allowing up to six mismatches to the guide sequence (Yin et al., 2019; Zhang et al., 2021), we found that the total number of off-target translocation sites in both days 14 and 30 was slightly lower for sgRNA3 compared to sgRNA4 (2 vs 5 and 2 vs 6, respectively), (Table S6, Figure S1f). Notably, all normalized off-target translocations for both guides were not located in oncogene regions nor were they located in exons (Table S7). Furthermore, there was no overlap in translocation sites between 14 and 30 days in sgRNA3 (Figure S1g), indicating no recurrent translocation "hotspots" for this guide. sgRNA4 had three overlapping translocated sites found in both the 14 and 30 days, in intronic and intergenic regions that are not known oncogenes (Figure S1g, Table S6).

Table 3
PEM-seq editing scores for sgRNAs 3 and 4. Sample d14 = donor 2407, 14 days; Sample d30 = donor 2407, 30 days.

sgRNA-sample	sgRNA3-d14	sgRNA3-d30	sgRNA4-d14	sgRNA4-d30
Editing efficiency	63.8 %	53.9 %	87.1 %	82.2 %

To summarize our findings, sgRNA4 provides more efficient editing compared to sgRNA3. However, we found sgRNA3 as the most promising alternative for the production of edited hTregs for clinical applications since it presents the safest editing outcome that is manifested by stronger on-target vs. off-target ratio and fewer off-targets overall. Therefore, we continued our further evaluations using sgRNA3.

3. Protocol optimization for the preparation of SRC-3 KO hTregs

The process of preparing genetically edited T cells involves multiple critical steps, including stimulation, genetic editing, and expansion. The order in which these steps are performed can possess a significant impact on key characteristics of the final product, such as cell count, viability, editing efficiency and population homogeneity. There are several published procedures for CRISPR-Cas9-based gene KO of T cells, including some that have implemented this technology for clinical development (Stadtmauer et al., 2020; De Castro et al., 2024). Given the modular nature of the multi-step processes involved in preparing genetically edited cell therapies, we sought to adjust the steps in the search for an optimal procedure. Four different protocols were tested in order to identify the optimal method for preparing genetically-edited hTregs (Fig. 2a).

Protocols 1 and 4 represent a procedure in which the stimulation of the cells takes place first followed by RNP electroporation (gene editing) and expansion of the cells. In protocol 1, after the electroporation step the cells are removed from TCR-stimulation, while in protocol 4 the stimulation continues for an additional two days after electroporation.

In protocols 2 and 3, the isolated cells were immediately subjected to electroporation, after which they allowed to recover for 30 minutes in a pre-warmed Treg media, followed by TCR-stimulation. After the stimulation, the cells are cultured in an anti-CD3/-CD28-free environment for the remainder of the culturing period. The key difference between the two protocols is in the duration of the stimulation: four days in protocol 2 and ten days in protocol 3.

As evidenced by gene and protein expression analyses (Fig. 2b), all protocols result in an effective gene-editing with a seven-to-eight-fold expansion of viable edited cells after 14 days (Fig. 2c). Achieving peak cell expansion at earlier time points suggests the potential for an accelerated production process, which is a highly valuable attribute in cell therapy production in general (Ayala Ceja et al., 2024). Protocol 3 showed the lowest fold expansion on day 10, likely due to the delayed stimulation step. In contrast, for protocols 1 and 2 the expansion rate of the cells achieved its peak on day 10. The simplicity of a protocol is a highly desirable feature, particularly when considering its transfer to GMP production. For this reason, we prioritized protocol 2 over the other three protocols, as it represents the most straightforward approach, with both nucleofection and stimulation occurring

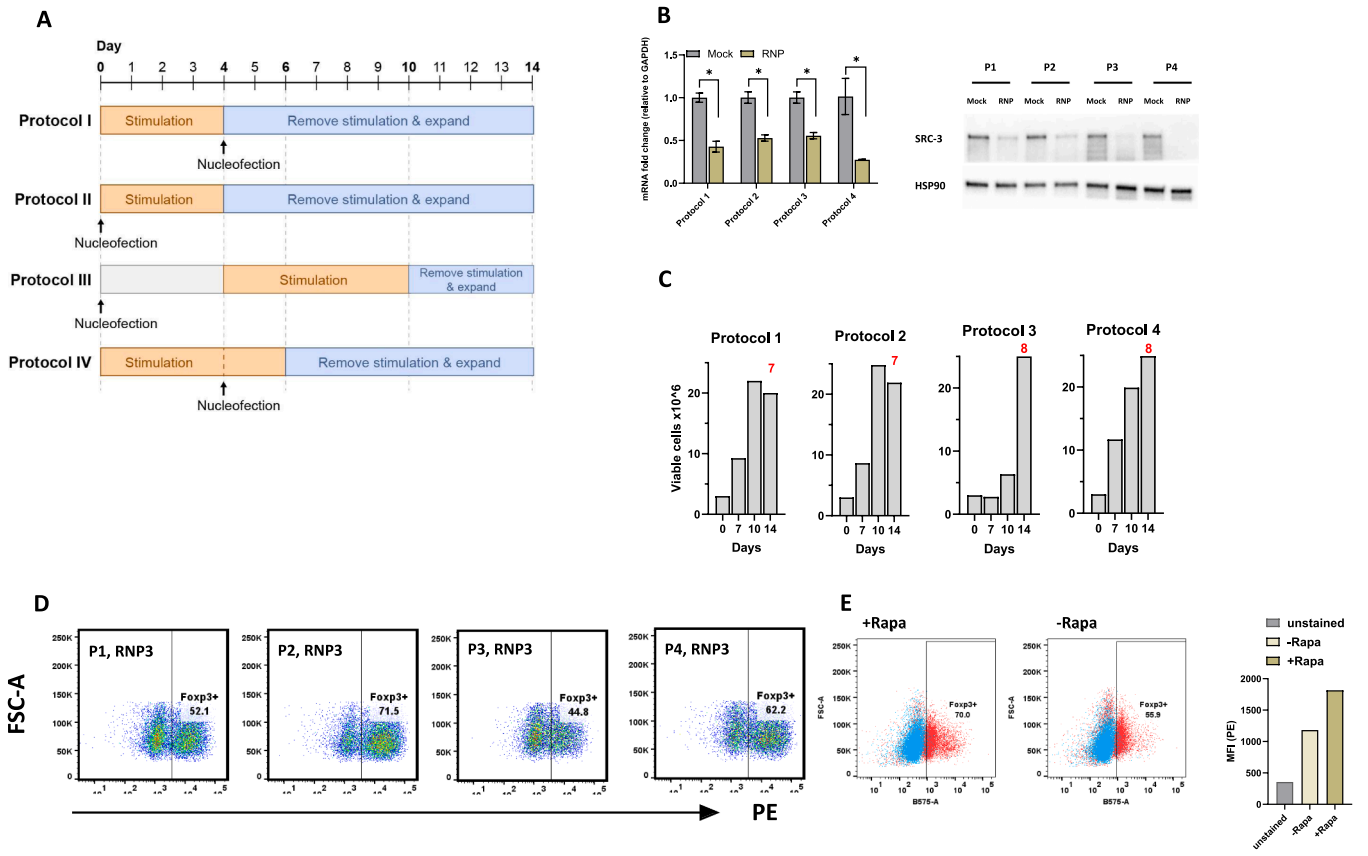

Fig. 2. The portion of Foxp3 + cells produced by protocols 1–4 (D). Histogram (left and middle) and MFI (right) representation of the portion of Foxp3 + edited Tregs when cultured with or without rapamycin. Representative data of at least two independent experiments showing similar results (E).

immediately after cell isolation. Notably, protocol 2 also yielded the purest hTreg population (Fig. 2d, S2a).

IL-2 is an essential cytokine in the culture media for Tregs. Indeed, when we compared hTreg cultures with or without IL-2 we found that in the absence of IL-2, cell viability and proliferation sharply declined (Figure S2b). Importantly, when the edited hTregs were expanded in the presence of IL-2 and then deprived of its supply, they stopped proliferating, which manifested in a decrease in cell counts (Figure S2c). The requirement of edited hTregs for an IL-2-rich environment for their steady proliferation, suggests a low probability of hyper-proliferation of these cells post-ACT.

Rapamycin is commonly added to Tregs culture media, since its addition increases the portion of Tregs in the final bulk expanded cell culture (Fraser et al., 2018). However, exposure to rapamycin can slow down the overall proliferation rate of all T cells. We therefore compared the proliferation rate and the portion of hTregs when the edited cells were cultured with or without rapamycin. As expected, rapamycin did slow down the proliferation rate of the overall population of the cells (Figure S2d), but it meaningfully increased the hTreg portion in the culture (Fig. 2e), thereby justifying its inclusion in the culturing media during production.

Since Cas9 is an essential substance for the production of the edited Tregs, rather than a part of the cell therapy in itself, residual Cas9 in the final cell therapy product by definition represents a manufacturing impurity and can introduce an unpredictable immunogenic risk factor. However, there is an absence of strict regulatory guidelines on residual Cas9 limits imposed by US Food and Drug Administration (FDA). We found that Cas9 levels declined over the culturing period, reaching < 1 fg/cell at the time of harvest (Figure S2e), that according to previously published clinically relevant data, is considered safe (Stadtmauer et al., 2020; Hu et al., 2021).

4. Scale up and cryopreservation of the final product

To increase the expansion rates of edited hTregs we used protocol 2 for the production of SRC-3 KO hTregs while utilizing a Gas-permeable Rapid Expansion (G-Rex) device (Vera et al., 2010) instead of a standard culture dish. A silicone membrane at the base of the G-Rex flask allows for O_2 and CO_2 to be exchanged, which drives uniform distribution of nutrients and dilution of metabolic waste in the growing population of cells. Therefore, this gas-permeable membrane can support an increase in the density T cells, without the need of frequent medium changes (Abou-el-Enein et al., 2021). These features of gas-permeable bioreactors not only improve the expansion of a T cell product but also decrease the intervention required for the maintenance of the culture, overall resulting in a more efficient and simple procedure which is optimal for GMP production. Indeed, in G-Rex devices we achieved a 25–40-fold expansion rate of the edited hTregs after 14 days, which is three to five-fold higher compared to expansion in a standard culture dish (Fig. 3a). Inclusion of IL-7 and IL-15 cytokines in the culture media increased the proliferation of the edited hTregs even more (Figure S3a). However, in order to maintain a low-complexity culture media, we did not include these cytokines in the final media recipe. Overall, the use of G-Rex bioreactors demonstrates the capability for scalable production of the hTreg therapy in a GMP-compatible setting. Future media optimization, where maximal expansion is prioritized over media simplicity, may involve the inclusion of additional cytokines such as IL-7 and IL-15 to enhance hTreg proliferation.

Functional evaluation of the edited cells is important both to gain insight into the activity of these cells and to potentially serve as a release criterion for the final cell therapy product. To assess the functionality of the SRC-3 KO hTregs generated in this study, we performed IFNγ release profiling using an ELISA assay. The rationale for this approach was

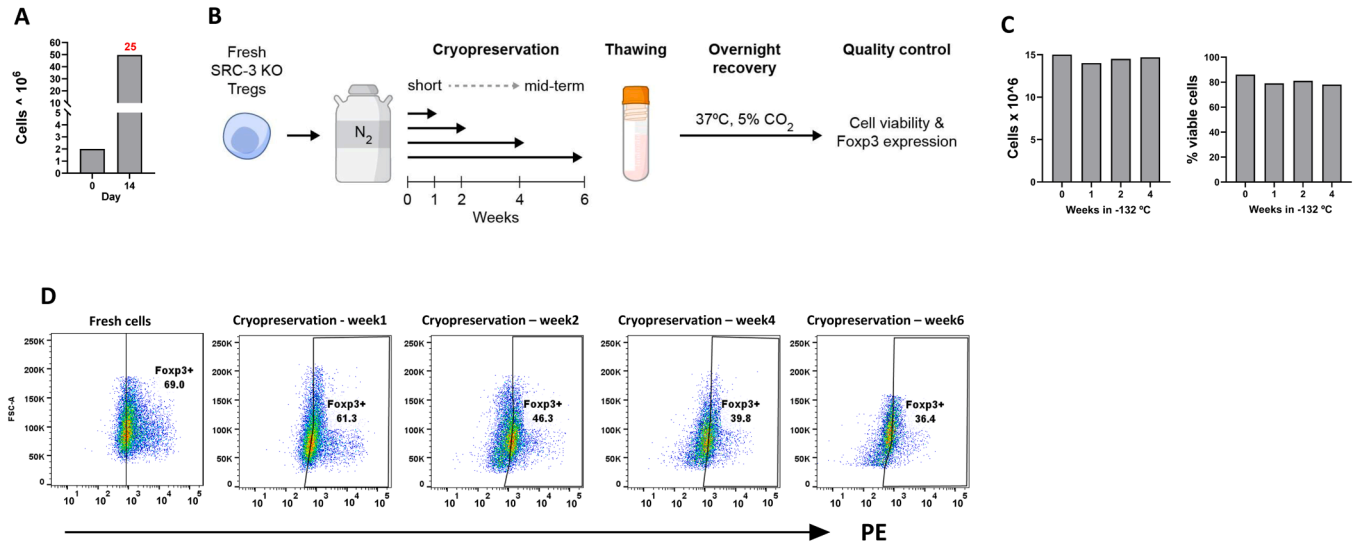

Fig. 3. Expansion of SRC-3 KO Tregs in G-Rex. Representative data of at least two independent experiments showing similar results (A). Schematic presentation of the cryopreservation process (B). Cell count (left) and viability (right) before (week 0) and after (weeks 1, 2, 4, 6) cryopreservation. Representative data of at least two independent experiments showing similar results (C). Foxp3 expression in SRC-3 KO Tregs over the time course of cryopreservation. The samples were analyzed using the gating strategy shown in Fig. S3C, with Foxp3 gates determined relative to the internal reference control specific to each sample (see Fig. S3d). Representative data of at least two independent experiments showing similar results (D).

based on our previous findings demonstrating that infiltration of SRC-3 KO Tregs into the TME is associated with elevated IFNγ production and enhanced anti-tumor immunity (Han et al., 2023). Consistent with our prior observations, the edited hTregs displayed higher release of IFNγ compared to WT counterparts in vitro (Figure S3b), supporting the notion that SRC-3 KO Tregs acquire a functional phenotype relevant to their intended therapeutic mechanism.

Cryopreservation is an essential component in the logistic chain that supports the overall production and supply of cell therapies, since it enables the storage of the final cell therapy product until it is needed to be delivered to the clinic (Meneghel et al., 2020). Cryopreservation allows for large-scale production and bio-banking of ready-to-use cell therapies, eliminating the reliance on donor availability, which is key in cases when time is a critical factor. Moreover, in cases when a cell therapy is produced in excess, cryopreservation ensures it will be available on demand for future use, which also minimizes product waste and lowers production costs. However, cryopreservation of cellular products can present technical challenges related to batch-to-batch variability, cell viability, recovery and function. These challenges are even more pronounced with Tregs due to the fragility and unstable expression of the Treg marker FOXP3 (Elkord, 2009; Golab et al., 2013). To evaluate the impact of cryopreservation on the final cell product, we cryopreserved the SRC-3 KO hTregs generated by protocol 2 and thawed after one, two, four and six weeks, which represents short- to mid-term cryopreservation (Fig. 3**b**). After thawing, the cells were allowed to recover overnight followed by cell viability and FOXP3 expression evaluation. Cell viability and cell count of the thawed SRC-3 KO hTregs at all time points were virtually the same as fresh cells (Fig. 3**c**). However, expanded fresh SRC-3 KO hTregs showed nearly 70 % FOXP3 expression, which was gradually reduced over the time of cryopreservation, reaching ~50 % of that original FOXP3 levels on week six (Fig. 3d, S3c, S3d). Instability of Treg cell marker expression as a result of cryopreservation is not unexpected according to previously reported data (MacDonald et al., 2019; Gołąb et al., 2018). Importantly, short-term cryopreservation (*i.e.* one week), which is most important for the very fundamental logistic needs such as delivery from production site to clinic, causes less than 10 % drop in FOXP3 expression, implying minor phenotype change. Moreover, we found that allowing the edited hTregs a longer recovery period leads to FOXP3 expression levels that closely match those found in fresh cells (Figure S3e). Overall, our cryopreservation experiments show that SRC-3 KO hTregs can be cryopreserved for short-term periods without bringing about major changes in FOXP3 expression. Longer cryopreservation periods might result in significant reduction of FOXP3 levels, which can be partially reversed by restimulation of the cells after thawing and allowing for longer recovery phase.

5. Materials and methods

Cells and cell cultures: hTregs were isolated from leukopack bags (received from Charles River, Northridge, CA,USA, See donor related information summary in Table S8) on MultiMACS Cell24 Separator instrument (Miltenyi Biotec, MD, USA), using human peripheral blood mononuclear cells (PBMC) isolation kit (Miltenyi Biotec, Catalog #120051115), human CD8 + and CD19 + depletion MicroBeads (Miltenyi Biotec, Catalog #130–045–201 and Catalog #130–050–301 respectively) and human CD25 positive selection MicroBeads II (Miltenyi Biotec, Catalog #130–092–983), according to manufacturer's procedures. In short, a bulk CD4 + T cell population was obtained by isolating total PBMCs from leukopaks and subsequent depletion of CD8 + and CD19 + cells. hTregs were then isolated by positive selection of CD25 + cells from the bulk CD4 + T cell population and cultured in a hTreg culture media.

hTregs were isolated from buffy coats received from Gulf Coast Regional Blood Center, TX, USA See donor related information summary in Table S8). A Needleless IV Bag Access Device (ICU Medical, Inc., CA, USA) attached to a 60 mL syringe (BD, Catalog #309653) was used to transfer the blood to 50 mL conical tubes. RosetteSep Human CD4 + T Cell Enrichment Cocktail (STEMCELL Technologies, Catalog #15062) was then added to the blood sample to deplete all non-CD4 + T cells. Density-gradient based separation of the CD4 + cell population was achieved using SepMate 50 mL conical tubes (STEMCELL Technologies, Catalog #85450) layered with Lymphoprep (STEMCELL Technologies, Catalog #07851). Next, ACK Lysing Buffer (Quality Biological, Catalog #118–156–101) was used to remove any contaminating red blood cells. Finally, the purified population of CD4 + T cells was incubated with CD25 MicroBeads II (Miltenyi Biotec, Catalog #130–092–983). This suspension was passed through LS columns (Miltenyi Biotec, Catalog #130–042–401) attached to the QuadroMacs magnet (Miltenyi Biotec, MD, USA). The CD4 + CD25 + cell population retained within each

magnetic column was eluted with FACS buffer using the LS Column plunger.

For the preparation of hTreg culture media, 45 % Advanced RPMI 1640 media (Gibco, Catalog # 12633), 45 % EHAA (Click's Media, Irvine Scientific Catalog #9195), and 10 % heat inactivated human serum albumin (Valley Biomedical Catalog #HP1022) were mixed and supplied with 2 mM L-Glutamine (HyClone, Catalog # SH30034.1). If not indicated otherwise, the media was also supplied with 500 U/mL IL-2 (R&D System, Catalog #BT-002-GMP-050) and 100 nM Rapamycin (Selleckchem, Catalog # S1039). When mentioned, IL-7 and IL-15 were used at a concentration of 10 ng/mL.

For the IL-2 deprivation experiment, hTregs were edited and cultured according to protocol 2 procedure. At the end of the protocol 2 culturing period (day 14), 2 M cells were equally split into two groups and cultured for another 14 days in the hTreg culture media with or without IL-2. Cell counts were performed on day 21 and day 28.

Jurkat cells were obtained from the AtCC and cultured in full RPMI, supplied with pen strep.

Guide design: sgRNAs were designed using the Synthego Design Tool. The algorithm prioritizes guides which specifically target early exons to provide the highest likelihood of causing a functional knockout. The algorithm then targets common exons to knockout all transcripts, or as many transcripts as possible, and assigns a score to each guide (based on Doench et. al (Doench et al., 2016).) to maximize activity and minimize off-target effects. sgRNAs 1 and 2 had the top two scores. sgRNAs 3 and 4 were scored lower according to this algorithm, since they target later exons.

Cryopreservation: Cell samples for cryopreservation were prepared according to protocol 2. At the end of the culturing period, the cells were harvested, centrifuged and the supernatant was removed. The cell pellet was resuspended in a cold cryopreservation media comprised of 90 % fetal bovine serum (FBS) and 10 % dimethyl sulfoxide (DMSO) to generate a 10^7 cells/mL cell suspension. The cell suspension was distributed between 1 mL cryotubes, which were then transferred to the cryo container (Mr. Frosty Freezing Container, Fisher Scientific, PA, USA) containing isopropanol at −80°C, and 24 hours later the cryotubes were transferred for cryopreservation in liquid nitrogen. Cryopreserved samples were thawed at different time points in a 37°C water bath, followed by centrifugation, removal of the DMSO-containing supernatant, resuspension in hTreg culture media, transfer into culture dishes and incubation at 37°C with 5 % CO_2. The cells allowed to recover for 24 hr after which the cells were counted, cell viability was evaluated, and cells were subjected to flow cytometry analysis.

Longer recovery period involved three days recovery with anti-CD3/-CD28 stimulation, media change and three additional days of stimulation-free expansion. After the prolonged recovery period the cells were subjected to cell viability evaluation, cell count and flow cytometry analysis.

Real Time Quantitative Polymerase Chain Reaction (RTqPCR): RNA was extracted from cells using RNeasy kits (Qiagen) according to manufacturer's protocol. 2 μg of total RNA was used for cDNA synthesis using a VILO Superscript cDNA Synthesis Kit (Invitrogen). Probe-based RTqPCR was performed using commercial probes (Universal Probe Library probes – Roche) for the housekeeping gene (*GAPDH*), custom designed probes (Custom TaqMan MGB Probes, Applied Biosystems) for the *NCOA3* gene (with an exception for Fig. 1a where for the *NCOA3* mRNA expression levels a commercial probe was used) (Tables S9, S10) and TaqMan Universal Master Mix (Applied Biosystems), on a Step One Plus Real-Time qPCR machine (Applied Biosystems). Relative mRNA expression levels of *NCOA3* were calculated using the ΔΔCT method with normalization to a housekeeping gene (*GAPDH*). Each result is represented by SD of three technical replicates.

Immunoblotting: Whole cell lysates were obtained using RIPA lysis and extraction buffer (ThermoFisher), according to manufacturer's protocol. Briefly, 30 min ice-cold incubation of cells with extraction buffer followed by 15 min 15, 000 rpm centrifugation at 4°C. The tubes were carefully removed from the centrifuge, supernatants were collected and protein concentrations were measured using Pierce bicinchoninic acid assay (BCA) protein assay kit (ThermoFisher). Then, protein-containing supernatants were added with 25 % v/v Laemmli sample buffer (BioRad) containing 10 % 2-mercaptoethanol and boiled for five min at 95°C. Protein samples were loaded and run on 4–20 % precast polyacrylamide gels (Mini-PROTEAN TGX Precast Protein Gels, Bio-Rad). Gels were washed and then transferred to nitrocellulose membranes using an iBlot Gel Transfer Device (ThermoFisher). The nitrocellulose membranes were blocked by soaking for 60 min in 5 % nonfat dry milk in PBS-Tween blocking buffer and then exposed to primary antibodies - in the same buffer - by over-night incubation at 4°C (Table S11), followed by thorough washing with PBS, and incubation with a relevant horseradish peroxidase (HRP)-conjugated secondary antibody for 60 min at room temperature. Membranes were then washed with PBS and protein bands were detected by either Pierce enhanced chemiluminescence (ECL) kit, SuperSignal West Pico PLUS kit or SuperSignal West Femto PLUS kit (all ThermoFisher) in a V3 Western Workflow (BioRad).

Flow cytometry: Cells were washed with PBS and centrifuged. Pellets were then rinsed in 100 μL/sample cell staining buffer (Bio-Legend) and incubated on ice for 45–60 minutes with fluorophore-conjugated Abs for cell surface markers (Table S12). For live/dead discrimination 1 μl Near IR 780 dye (Invitrogen, L34994a) was added. Cells were then washed with PBS and either resuspended in cell staining buffer or subjected to an extra step of FOXP3 staining using the FOXP3 transcription factor staining buffer set (Invitrogen) according to manufacturer's protocol and then resuspended in cell staining buffer. All cell samples were passed through a 0.40 μm filter prior to loading onto a LSRII cell analyzer (Becton and Dickinson). Negative controls for all fluorophores were performed using the fluorescence minus one (FMO) method. Data analysis was performed using the Diva software package (Becton and Dickinson). Final data analysis and visualization were performed with FlowJo_v10 software. Mean fluorescent intensity (MFI) graphs were generated with Prism (GraphPad Software, Inc.).

CRISPR KO: For the formation of an RNP complex synthetic single guide RNA (sgRNA) (Synthego) was brought to 200 μM concentration by reconstitution in sterile TE buffer followed by 15 min incubation with recombinant NLS-SpCas9 protein (IDT; 1081059) at 37°C at a Cas9:RNA ratio of 1:2.5 (Table S13). Cells were prepared for nucleofection by washing with PBS and resuspended in 100 μl SE (Jurkat cells) or P3 (hTregs) buffer (Lonza; V4XC-1012 or V4XP-3024 respectively). RNP complex was added into the cell suspension to form the nucleofection mix, which was then transferred into a 100 μl reaction cuvette (4D-Nucleofector System, Lonza). The reaction cuvette was loaded into the nucleofector and either program CL-120 (Jurkat cells) or FI115 (hTregs) were applied. Immediately after nucleofection the mixture was transferred into a pre-warmed culture media.

Guide SEQ analysis: Cell samples for Guide SEQ analysis were generated according to protocol 2, with some modifications; hTregs were nucleofected simultaneously with RNP complex and dsODN (IDT, IA, USA), which serves as the Guide seq marker. Donors 2330 and 2322 were harvested five days after nucleofection while Donor 2424 was harvested on day 14. After harvesting, hTregs (8×10^6) were centrifugated and kept at −80 °C up to shipment day. Guide seq analysis was done by Creative Biogene Ltd (NY, USA) according to previously published procedure (Tsai et al., 2015). Briefly, genomic DNA was randomly fragmented to 500 bp using E220 Focused-Ultrasonicator (Covaris). Following end-repair, A-tailed and ligation, two rounds of PCR were performed to amplify the fragments carrying the dsODN sequence. The DNA library was then sequenced on MGI 2000 platform with 150-bp paired-end reads. Demultiplexing and data quality filtering were performed as follows: Samples were demultiplexed using fastp (https://github.com/OpenGene/fastp?tab=readme-ov-file#simple-usage) allowing for one mismatch on each index. Data was filtered as follows: Minimum base quality 20, sliding window of 4 bp, minimum

read length of 50 bp, proportion of unqualified bases < 10 %. Analysis of GUIDEseq was performed using the GUIDEseq software package (https://github.com/aryeelab/guideseq). NextEra 8 bp dual indexes with an 8 bp UMI were used to tag samples (Tsai et al., 2015). Hg38 was used as the reference genome, with default parameters, using a search radius of 10 bp for Cas9. The maximum number of mismatches allowed to report a sequence-matched off-target was set to six. Briefly, data for each sample was consolidated using UMI indexing to remove PCR duplicates, then mapped using Burrows-Wheeler Aligner (BWA) to reference genome to identify off-target editing events.

TIDE analysis: Genomic DNA was isolated from 100,000 cells (Donors 2407 and 2342) cultured and nucleofected according to protocol 2 using PureLink Genomic DNA kit (Invitrogen, CA USA) following manufacturer's instructions. PCR amplicons spanning the sgRNA genomic target sites were generated using the OneTaq Hot Start Master Mix (New England Biolabs, MA, USA) with the following primer pairs: gRNA3_fw: 5′-CAGTAGTGCCATCACAGCTCAC-3′; gRNA3_rv: 5′-AGCCCATAGTTGTTGTTCTGGT −3′; gRNA4_fw: 5′-CCAGAACAACAACTATGGGCT-3′; gRNA4_rv: 5′-AGGACCCCTTTGATTCTCTGC −3′. Purified PCR products were Sanger-sequenced (DNA Sequencing Core, Baylor College of Medicine, Houston, TX) using both PCR primers. Each sequence chromatogram was analyzed with the TIDE online software tool (http:// tide.nki.nl). Genomic DNA from the mock-nucleofected sample (nucleofection without RNP) was used as a reference sequence. Default parameters were used as recommended by Brinkman et al (Brinkman et al., 2014)., with maximum indel size range of 10 bp and maximum sequence segment decomposition window for sufficient coverage. All Sanger sequences were high quality so no parameter adjustments were needed.

PEM-seq analysis: Cell samples for PEM-seq analysis were generated according to protocol 2 with the following modification: hTregs from Donor 2407 were harvested 14 and 30 days after nucleofection. After harvesting, hTregs were centrifugated and kept at −80 °C up to shipment day. PEM-seq analysis was done by Creative Biogene Ltd (NY, USA) implementing a previously described methodology (Yin et al., 2019). 10^7 edited hTregs and unedited (mock nucleofected) control cells were used to extract genomic DNA. 10 μg of gDNA was used for further process. First, the gDNA was sheared using the E220 Focused-Ultrasonicator (Covaris) to obtain 300–700 bp fragments. Then, a target-specific biotinylated primer was used for primer extension. The biotinylated single-stranded DNA was enriched with Dynabeads MyOne Streptavidin C1 (Thermo Fisher) and then ligated with a 'bright adaptor' to facilitate exponential amplification of the target fragments. 'On-beads' nested PCR was performed and followed by size selection and another round of PCR. The library was sequenced on a MGI 2000 platform. Demultiplexing and data quality filtering: Samples were demultiplexed using fastp (https://github.com/OpenGene/fastp?tab=readme-ov-file#simple-usage) allowing for one mismatch on each index. Data was filtered as follows: Minimum base quality 20, sliding window of 4 bp, minimum read length of 50 bp, proportion of unqualified bases < 10 %.

PEM-seq analysis: For the analysis of PEM-seq data, the PEM-Q software package (https://github.com/liumz93/PEM-Q) was used with default parameters. NextEra 8 bp dual indexes with a 12 bp in-line UMI were used to tag samples. Briefly, the pipeline works as follows: Illumina adaptor sequences were trimmed using CutAdapt. Mapping was performed with BWA using Hg38 as the reference genome, and PCR duplicates were removed with default parameters. Translocation hotspots were identified and further filtered. Filtering criteria used to define off-target sites were: 1) sRNA alignment within a + -50bp window around the junction site and 2) minimum number of reads > =3. 3) Maximum number of mismatches allowed to report a sequence-matched off-target translocation event was set to 6.

IFNγ ELISA assay: hTregs were isolated from donors 2424, 2501 and D1a as described above and subjected to empty or sgRNA3 RNP nucleofection and culture according to protocol 2. Five million cells per well were plated on a 6-well plate for either empty- or sgRNA3 RNP-nucleofected group. 500 μl media was aliquoted from the cultures 8, 24 and 48 hours after TCR stimulation. Media samples were kept at −20 °C until the performance of the ELISA assay. The assay was performed using the Quantikine® ELISA human IFNγ immunoassay (R&D system, #DIF50C) according to the instructions provided by the manufacturer. The reads were collected from TECAN Infinite M200 plate reader.

6. Summary and discussion

Due to their pivotal role in modulation of immune responses, the therapeutic applications of Tregs have gained a growing interest (Bluestone et al., 2023; Raffin et al., 2020). Current Treg-based therapies, and recent developments in the field are mostly focused on autoimmune diseases and organ-transplantation applications. However, the centrality of Tregs to the ability of tumors to evade immunosurveillance makes them obvious targets in cancer therapy. Indeed, immune checkpoint inhibitors, which have significantly impacted cancer treatment, target immunosuppressive pathways that are partly regulated by Tregs. However, clinical applications in which Tregs represent a direct cellular target are yet to be developed. In our recent publication we demonstrated that genetically edited Tregs are capable of orchestrating an enhanced immune response that leads to eradication of aggressive solid tumors in syngeneic mice models (Han et al., 2023). According to this publication, cKO of the *NCOA3* gene in Tregs brings about a marked shift in their function within the tumor microenvironment from immunosuppressive to immunostimulatory. These findings provide motivation for the development of a Treg-based cell therapy for solid tumors. The discovery and establishment of CRISPR-Cas technology as a robust tool for genetic manipulation has greatly enabled an expanded range of cell-based therapies. Recently, several reports have demonstrated the successful use of CRISPR-Cas9 for the genetic editing of T cells, including Tregs (Lam et al., 2021a, 2021b; Chen et al., 2024). However, the scarcity and fragility of Tregs still present a challenge in producing effectively edited Tregs of an adequate quantity and quality for clinical applications.

In the present work we described a protocol for generating *NCOA3* KO hTregs, while focusing on editing efficiency with minimal off-target edits, cell expansion and cell viability. Of note, it has been demonstrated that for immunosuppressive therapies in some cases antigen-specific Tregs are more effective than polyclonal Tregs (Bittner et al., 2023). However, the use of the SRC-3 KO Treg approach is unique, as it utilizes edited Tregs to activate an immune response rather than to suppress immunity. We have found no evidence indicating that antigen-specificity is required for efficacy in this context (Han et al., 2023). Therefore, it allows us to avoid the additional complexity of generating antigen-specific clones and thereby simplifying the overall process. Moreover, polyclonal Treg-cell products have shown efficacy in preclinical mouse models and are currently being evaluated in several early-phase clinical trials (Bittner et al., 2023). Nonetheless should antigen specificity be necessary, this protocol could be readily adapted by incorporating existing strategies such as in vitro antigen-specific expansion or TCR engineering (Bittner et al., 2023; Sakaguchi et al., 2023).

After a preliminary assessment of four different sgRNAs, we proceeded to further evaluate two sgRNAs that target the most important exons of the *NCOA3* gene, sgRNAs 3 and 4. Although RNPs of both sgRNAs effectively knocked out SRC-3 in hTregs, sgRNA4 possessed superior efficiency compared to sgRNA3. However, examination of the off- vs on-target editing using two orthogonal sequencing methods, revealed that sgRNA3 has considerably higher on:off target ratio, with 96 % on-target reads compared to 55 % on-target reads of sgRNA4. This effect of increased off-target activity associated with sgRNA4 was found in all donors and all timepoints examined. Furthermore, off-target chromosomal translocations in samples from two different time points (days 14 and 30) were fewer for sgRNA3. Indeed, there were two distinct

hotspot locations on chromosome 2 that underwent both translocation and off-target editing found in sgRNA4. Interestingly, these sites are relatively near to one another on the chromosome (~600 kb), and likely undergo a certain percentage of inversions and subsequent deletions as well. The strongest off-targets were 3 nucleotide mismatches from the guide, which would explain why they were so strongly edited. This emphasizes the importance of stringent filtering in guide-design for potential off-targets *in silico*. Importantly, no overlap in translocation sites were found between the two time points for sgRNA3, indicating no recurrent translocation hotspots. Notably, for both sgRNAs neither unintended edits nor chromosomal translocations (above the 0.1 % relative editing threshold) were observed within exonic regions, and only one target was found in the intron of an oncogene/TSG in both guides at very low relative editing levels (<0.2 %). This suggests a low risk of malignant transformations associated with CRISPR-Cas9 KO of *NCOA3* when using these sgRNAs, which is a critical consideration for the long-term safety of a cellular therapy. Follow-up of off-target sites of interest is recommended, with methods such as Rhamp-Seq, to validate the off-targets, on sites passing LOD filters of 0.1 %. Overall, both sgRNAs 3 and 4 effectively KO *NCOA3*, with sgRNA4 showing higher KO efficiency, but at the same time possessing a significantly higher risk of inducing transformative mutations due to a higher number of off-target cuts. Thus, the decision came down to balancing maximal editing efficiency against the need for a safer cell therapy product, which ultimately leads to a compromise on editing efficiency for a better safety profile. On-target editing efficiency verses precision is a common challenge in CRISPR editing, and high-fidelity Cas9 enzymes typically have reduced activity to achieve more precise editing, although recent high-fidelity enzymes are bridging this gap (Vos et al., 2024). Finally, sgRNA3 still achieves an effective KO of *NCOA3*, leading us to proceed with it, sacrificing some editing efficiency in favor of minimizing off-target effects to prioritize safety and maintain genome integrity.

The preparation of a genetically edited T cell therapy is a modular process involving several key steps. To evaluate how the order of these steps affects the quality and quantity of the Treg product, we designed four distinct procedures, each varying in the sequence of the main steps: stimulation, nucleofection, and stimulation-free expansion phase. While the overall expansion rates at the final time point were similar across the four protocols, protocols 1 and 2 achieved peak fold expansion at an earlier time point. Additionally, protocol 2 represents the simplest procedure, which is a favorable feature when considering production under GMP conditions. Importantly, in protocol 2 TCR stimulation takes place immediately after nucleofection, which guarantees minimal molecular and phenotypic changes of the Tregs prior to their subjection to the desired genetic modification (Morath et al., 2024). Moreover, performing the nucleofection prior to TCR activation has a lower potential for chromosomal loss (Tsuchida et al., 2023), which is a major genotoxicity concern in clinical applications of CRISPR-Cas gene-editing technology (Sheridan, 2021). Of note, protocol 2 produced the highest number of FOXP3-expressing SRC-3 KO hTregs, likely indicating that nucleofection prior to TCR stimulation better preserves the parental phenotype of the edited T cells. Importantly, HELIOS is frequently used alongside FOXP3 for more refined identification of Treg population. However, while HELIOS is predominantly expressed by Tregs, only a fraction of Tregs express this marker (Sebastian et al., 2016; Thornton et al., 2019). Therefore, in this study, we deemed HELIOS non-essential for the identification of the final SRC-3 KO Treg cell product, especially considering that our previous work ultimately relied on FOXP3 expression to generate conditional SRC-3 KO (Han et al., 2023). Furthermore, Treg-Specific Demethylated Region (TSDR) methylation analysis would further enhance the characterization of the Treg cell product. In this study, we relied on complementary measures, including $CD4^+CD25^+$ enrichment, FOXP3 expression analysis post-editing, and functional assessment through IFN-γ profiling, to support the stability and intended functionality of the edited Treg phenotype. However, TSDR methylation analysis remains a valuable approach for further confirming Treg lineage stability and will be considered in future studies.

We performed evaluation of cell viability and preservation of the Treg marker expression – FOXP3 – after recovery of the SRC-3 KO hTregs from cryopreservation. In all the tested timepoints, the cells retained their viability and cell counts that were virtually the same as for fresh cells. Expression of the Treg phenotype marker FOXP3 after short-term cryopreservation (one week) slightly reduced relative to fresh cells. However, during the course of time FOXP3 expression continued to drop, reaching less than 50 % FOXP3 + expressing population on week six compared to fresh cells. Importantly, we found that a longer recovery with restimulation of the cells following an extended cryopreservation period (>six weeks), restores FOXP3 expression levels and enables the expansion of edited Tregs. Our data suggest that short-term cryopreservation of the final Treg product, which in some cases is essential for the ability to deliver the cell therapy from the production site to the clinic, has virtually no deterioration effects on cell viability or cell count and only results in a slight decrease of FOXP3 expression. Although longer cryopreservation results in a negligible decrease of cell viability of cell count, a material drop in FOXP3 expression was observed. Of note, adjustments of recovery conditions after long-term cryopreservation, such as prolonging the recovery period and the re-stimulation of the Tregs, might bring about some recovery in the expression of FOXP3. Therefore, longer cryopreservation of edited Tregs, which are usually needed to secure availability of the cell product for post-immediate use, are optional but a change in the phenotypic composition of the bulk cell product should be considered.

Overall, we described a path towards selection of an optimized protocol for the generation of SRC-3 KO hTregs and evaluated the ability of their cryopreservation. Here we present a methodology that represents a comprehensive framework that balances editing efficiency while maintaining desired cell characteristics such as viability, expansion and minimal unintended editing events. The approach we used, that involved sgRNA selection through integration of bioinformatic analyses from two orthogonal sequencing methods alongside critical factors such as cell viability, expansion, and expression of key Treg phenotype biomarkers, can be broadly applied to similar genetic manipulations in hTregs with a perspective for cGMP production and clinical use.

Ethics

De-identified human cell leukapheresis and blood products were obtained from external entities, therefore the study was exempt from the Institute Review Board (IRB) review. Leukapheresis products (leukopaks) were obtained from Charles River, Northridge, CA, USA. Blood samples were obtained from the Gulf Coast Regional Blood Center. Both vendors certified that all donors provided informed consent for the use of donated cells for research purposes.

Funding

This work is partly supported by funding from the National Institutes of Health grants R01 HD07857 and R01 HD08188 (BWO) and from the Adrienne Helis Malvin Foundation to DML (DML) and CoRegen Inc.

CRediT authorship contribution statement

O'Malley Bert Williams: Writing – review & editing, Supervision, Funding acquisition, Conceptualization. **Moser Aiden Lynn:** Writing – review & editing, Data curation. **Ortal Shimon:** Writing – review & editing, Visualization, Methodology, Data curation, Conceptualization. **Gilad Yosef:** Writing – review & editing, Writing – original draft, Visualization, Supervision, Methodology, Data curation, Conceptualization. **Shoshana Cohen:** Writing – review & editing, Visualization, Methodology, Data curation. **Dean Adam:** Writing – review & editing, Project administration, Data curation. **Lonard David:** Writing – review & editing, Supervision, Funding acquisition, Conceptualization. **Dacso**

Clifford Clark: Writing – review & editing.

Declaration of Competing interest

CCD, YG, DML and BWO are paid consultants by and disclose an equity position in CoRegen, Inc. AMD discloses an equity position in CoRegen, Inc. The other authors declare that they have no conflicts of interest.

Acknowledgments

The authors acknowledge the graphic design assistance provided by Dr. Sandy R. Westermann (www.scigraphix.com).

Appendix A. Supporting information

Supplementary data associated with this article can be found in the online version at doi:10.1016/j.molimm.2025.05.019.

Data availability

Data will be made available on request.

References

Abou-el-Enein, M., et al., 2021. Scalable Manufacturing of CAR T Cells for Cancer Immunotherapy. Blood Cancer Discov. 2 (5), 408–422.
Ayala Ceja, M., et al., 2024. CAR-T cell manufacturing: Major process parameters and next-generation strategies. J. Exp. Med. 221 (2).
Bittner, S., Hehlgans, T., Feuerer, M., 2023. Engineered Treg cells as putative therapeutics against inflammatory diseases and beyond. Trends Immunol. 44 (6), 468–483.
Bluestone, J.A., et al., 2023. Opportunities for Treg cell therapy for the treatment of human disease. Front Immunol. 14, 1166135.
Brinkman, E.K., et al., 2014. Easy quantitative assessment of genome editing by sequence trace decomposition. Nucleic Acids Res. 42 (22), e168.
Chen, C., Wang, Z., Qin, Y., 2023. CRISPR/Cas9 system: recent applications in immuno-oncology and cancer immunotherapy. Exp. Hematol. Oncol. 12 (1), 95.
Chen, X., et al., 2024. CRISPR–Cas9 applications in T cells and adoptive T cell therapies. Cell. Mol. Biol. Lett. 29 (1), 52.
De Castro, V., et al., 2024. CRISPR-Cas gene knockouts to optimize engineered T cells for cancer immunotherapy. Cancer Gene Ther. 31 (8), 1124–1134.
Doench, J.G., et al., 2016. Optimized sgRNA design to maximize activity and minimize off-target effects of CRISPR-Cas9. Nat. Biotechnol. 34 (2), 184–191.
Elkord, E., 2009. Frequency of human T regulatory cells in peripheral blood is significantly reduced by cryopreservation. J. Immunol. Methods 347 (1-2), 87–90.
Ferreira, L.M.R., et al., 2019. Next-generation regulatory T cell therapy. Nat. Rev. Drug Discov. 18 (10), 749–769.
Fraser, H., et al., 2018. A Rapamycin-Based GMP-Compatible Process for the Isolation and Expansion of Regulatory T Cells for Clinical Trials. Mol. Ther. Methods Clin. Dev. 8, 198–209.
Gilad, Y., et al., 2024. Steroid receptor coactivators in Treg and Th17 cell biology and function. Front. Immunol. 15, 1389041.
Gilad, Y., Lonard, D., O'Malley, B., 2022. Steroid Receptor Coactivators-Their Role in Immunity. Front. Immunol. 13.
Golab, K., et al., 2013. Challenges in cryopreservation of regulatory T cells (Tregs) for clinical therapeutic applications. Int Immunopharmacol. 16 (3), 371–375.
Gołąb, K., et al., 2018. Cell banking for regulatory T cell-based therapy: strategies to overcome the impact of cryopreservation on the Treg viability and phenotype. Oncotarget 9 (11), 9728–9740.
Han, S.J., et al., 2023. Steroid receptor coactivator 3 is a key modulator of regulatory T cell–mediated tumor evasion. Proc. Natl. Acad. Sci. 120 (23), e2221707120.
Hu, Y., et al., 2021. CRISPR/Cas9-Engineered Universal CD19/CD22 Dual-Targeted CAR-T Cell Therapy for Relapsed/Refractory B-cell Acute Lymphoblastic Leukemia. Clin. Cancer Res. 27 (10), 2764–2772.
Kleinewietfeld, M., Hafler, D.A., 2014. Regulatory T cells in autoimmune neuroinflammation. Immunol. Rev. 259 (1), 231–244.
Lam, A.J., et al., 2021a. Optimized CRISPR-mediated gene knock-in reveals FOXP3-independent control of human Treg identity. bioRxiv, p. 2021.01.16.426937.
Lam, A.J., et al., 2021b. Optimized CRISPR-mediated gene knockin reveals FOXP3-independent maintenance of human Treg identity. Cell Rep. 36 (5), 109494.
Liang, S.-Q., et al., 2022. Genome-wide detection of CRISPR editing in vivo using GUIDE-tag. Nat. Commun. 13 (1), 437.
Liston, A., et al., 2024. Brain regulatory T cells. Nat. Rev. Immunol. 24 (5), 326–337.
Liu, Y., et al., 2022. PEM-seq comprehensively quantifies DNA repair outcomes during gene-editing and DSB repair. STAR Protoc. 3 (1), 101088.
Liu, Z., et al., 2008. Generation and validation of a mouse line with a floxed SRC-3/AIB1 allele for conditional knockout. Int. J. Biol. Sci. 4 (4), 202.
MacDonald, K.N., et al., 2019. Cryopreservation timing is a critical process parameter in a thymic regulatory T-cell therapy manufacturing protocol. Cytotherapy 21 (12), 1216–1233.
Machhi, J., et al., 2020. Harnessing regulatory T cell neuroprotective activities for treatment of neurodegenerative disorders. Mol. Neurodegener. 15 (1), 32.
Meneghel, J., Kilbride, P., Morris, G.J., 2020. Cryopreservation as a Key Element in the Successful Delivery of Cell-Based Therapies-A Review. Front Med (Lausanne) 7, 592242.
Miyara, M., et al., 2009. Functional Delineation and Differentiation Dynamics of Human CD4+ T Cells Expressing the FoxP3 Transcription Factor. Immunity 30 (6), 899–911.
Morath, K., et al., 2024. Activation-neutral gene editing of tonsillar CD4 T cells for functional studies in human ex vivo tonsil cultures. Cell Rep. Methods 4 (1), 100685.
Nikolai, B.C., et al., 2021. Steroid receptor coactivator 3 (SRC-3/AIB1) is enriched and functional in mouse and human Tregs. Sci. Rep. 11 (1), 3441.
Raffin, C., Vo, L.T., Bluestone, J.A., 2020. Treg cell-based therapies: challenges and perspectives. Nat. Rev. Immunol. 20 (3), 158–172.
Sakaguchi, S., Kawakami, R., Mikami, N., 2023. Treg-based immunotherapy for antigen-specific immune suppression and stable tolerance induction: a perspective. Immunother. Adv. 3 (1), ltad007.
Sebastian, M., et al., 2016. Helios Controls a Limited Subset of Regulatory T Cell Functions. J. Immunol. 196 (1), 144–155.
Sheridan, C., 2021. CRISPR therapies march into clinic, but genotoxicity concerns linger. Nat. Biotechnol. 39 (8), 897–899.
Simonetta, F., et al., 2010. Increased CD127 expression on activated FOXP3+CD4+ regulatory T cells. Eur. J. Immunol. 40 (9), 2528–2538.
Stadtmauer, E.A., et al., 2020. CRISPR-engineered T cells in patients with refractory cancer. Science 367 (6481).
Thornton, A.M., et al., 2019. Helios(+) and Helios(-) Treg subpopulations are phenotypically and functionally distinct and express dissimilar TCR repertoires. Eur. J. Immunol. 49 (3), 398–412.
Togashi, Y., Shitara, K., Nishikawa, H., 2019. Regulatory T cells in cancer immunosuppression — implications for anticancer therapy. Nat. Rev. Clin. Oncol. 16 (6), 356–371.
Tsai, S.Q., et al., 2015. GUIDE-seq enables genome-wide profiling of off-target cleavage by CRISPR-Cas nucleases. Nat. Biotechnol. 33 (2), 187–197.
Tsuchida, C.A., et al., 2023. Mitigation of chromosome loss in clinical CRISPR-Cas9-engineered T cells. Cell 186 (21), 4567–4582.e20.
Vera, J.F., et al., 2010. Accelerated production of antigen-specific T cells for preclinical and clinical applications using gas-permeable rapid expansion cultureware (G-Rex). J. Immunother. 33 (3), 305–315.
Vos, P.D., et al., 2024. Mutational rescue of the activity of high-fidelity Cas9 enzymes. Cell Rep. Methods 4 (4), 100756.
Yin, J., et al., 2019. Optimizing genome editing strategy by primer-extension-mediated sequencing. Cell Discov. 5 (1), 18.
Zhang, W., et al., 2021. In-depth assessment of the PAM compatibility and editing activities of Cas9 variants. Nucleic Acids Res. 49 (15), 8785–8795.